Vacancy-type defects induced by grinding of Si wafers studied by monoenergetic positron beams

Akira Uedono,[1] Yoriko Mizushima,[2,3] Youngsuk Kim,[3,4] Tomoji Nakamura,[2] Takayuki Ohba,[3] Nakaaki Yoshihara,[1] Nagayasu Oshima,[5] and Ryoichi Suzuki[5]
[1]*Division of Applied Physics, Faculty of Pure and Applied Science, University of Tsukuba, Tsukuba, Ibaraki 305-8573, Japan*
[2]*Devices & Materials Labs Fujitsu Laboratories Ltd., Atsugi, Kanagawa 243-0197, Japan*
[3]*ICE Cube Center, Tokyo Institute of Technology, Yokohama 226-8503, Japan*
[4]*Disco Corporation, Ota, Tokyo 143-8580, Japan*
[5]*Research Institute of Instrumentation Frontier, National Institute of Advanced Industrial Science and Technology, Tsukuba, Ibaraki 305-8568, Japan*

(Received 10 June 2014; accepted 16 September 2014; published online 2 October 2014)

Vacancy-type defects introduced by the grinding of Czochralski-grown Si wafers were studied using monoenergetic positron beams. Measurements of Doppler broadening spectra of the annihilation radiation and the lifetime spectra of positrons showed that vacancy-type defects were introduced in the surface region (<98 nm), and the major defect species were identified as (i) relatively small vacancies incorporated in dislocations and (ii) large vacancy clusters. Annealing experiments showed that the defect concentration decreased with increasing annealing temperature in the range between 100 and 500 °C. After 600–700 °C annealing, the defect-rich region expanded up to about 170 nm, which was attributed to rearrangements of dislocation networks, and a resultant emission of point defects toward the inside of the sample. Above 800 °C, the stability limit of those vacancies was reached and they started to disappear. After the vacancies were annealed out (900 °C), oxygen-related defects were the major point defects and they were located at <25 nm. © *2014 AIP Publishing LLC*. [http://dx.doi.org/10.1063/1.4896829]

I. INTRODUCTION

Three-dimensional (3D) integration technology is a candidate to extend Moore's law and solve issues caused by the scaling of metal-oxide-semiconductor structures which is approaching their physical limits.[1] The basic concept of 3D integration is to integrate more transistors into the same area by vertically stacking them. This is the trend of the semiconductor industry, and its driving force is increasing demands for highly functional and lightweight electronic products available at low cost. In 3D integration, three kinds of stacking approaches are used: chip-on-chip, chip-on-wafer, and wafer-on-wafer (WOW).[2–5] Among these methods, WOW bonding has the greatest potential to maximize throughput because of its simple process flow. For 3D-devices, their reliability, heat dissipation, and testing methodologies are current issues that must be resolved to enable 3D integration.[6,7]

Although WOW has several advantages, the main drawback of this method is the difficulty in maximizing the number of known-good-die combinations in the stacked wafers when the device wafer yield is not high enough. A key technology of the WOW method is wafer thinning, because a Si wafer less than 10 μm thick is used in this process. Extensive studies of wafer thinning have been carried out.[8,9] The process flow of wafer thinning mainly consists of coarse grinding, fine grinding, and chemical mechanical polishing (CMP) for stress relief. The major residual defects introduced during the grinding process are known to be dislocations and a thin amorphous layer.[10,11] Dislocations are major defects caused by Si deformation, and pure screw dislocations are the most important of these. It is generally accepted that Si undergoes phase transformation under the extremely high pressure introduced by the grinding process, where a transition from a diamond cubic to a metallic state β-Sn occurs. Since the metallic state is not stable at low pressure, it changes into an amorphous phase after the pressure is removed. In wafer thinning processes, a major concern is to obtain a wafer surface without those residual damages or with only the sort of damage that can be removed by subsequent processes. Many studies evaluating Si damage in relation to the thinning have been reported for conventional grinding conditions.[10–12] However, point defects such as vacancy-type defects are not well known because there was no technique to detect such defects. In addition, because the wafer thickness used in the WOW process is more than 10 times thinner than that of conventional wafers, detailed knowledge about residual defects introduced by grinding and their nature is crucial. Positron annihilation is a powerful technique for evaluating vacancy-type defects in semiconductors.[13,14] In the present study, we have used monoenergetic positron beams to probe defects introduced by the grinding of Si and their annealing behaviors.

When a positron is implanted into condensed matter, it annihilates with an electron and emits two 511-keV γ quanta.[13,14] The energy distribution of the annihilation γ rays is broadened by the momentum component of the annihilating electron-positron pair p_L, which is parallel to the emitting direction of the γ rays. The energy of the γ rays is given by $E_\gamma = 511 \pm \Delta E_\gamma$ keV. Here, the Doppler shift ΔE_γ is given by $\Delta E_\gamma = p_L c/2$, where c is the speed of light. A freely diffusing positron may be localized in a vacancy-type defect because

of Coulomb repulsion from positively charged ion cores. Because the momentum distribution of the electrons in such defects differs from that of electrons in the bulk material, these defects can be detected by measuring the Doppler broadening spectra of the annihilation radiation. The resultant changes in the spectra are characterized by the S parameter, which mainly reflects changes due to the annihilation of positron-electron pairs with a low-momentum distribution, and by the W parameter, which mainly characterizes changes due to the annihilation of pairs with a high-momentum distribution. In general, the characteristic value of S (W) expected for the annihilation of positrons due to their trapping by vacancy-type defects is larger (smaller) than that for positrons annihilated from the free-state. The lifetime of positrons trapped by vacancy-type defects increases because of the reduced electron density in such defects. Information obtained by measuring the lifetime spectra of positrons is useful for identifying vacancy-type defects.

II. EXPERIMENT

The samples investigated were 300-mm Si wafers grown by the Czochralski method. Details of the grinding method and the evaluations of residual defects using cross-sectional transmission electron microscope (X-TEM) and Raman spectroscopy are reported elsewhere.[15] The wafer was thinned in two stages; a grit size of #320 was used for coarse grinding and a grit size of #2000 for fine grinding, where the removed thicknesses for the coarse and fine grindings were 75 μm and 50 μm, respectively. The damaged subsurface was characterized by X-TEM. The sample was prepared by focused ion beam (FIB) milling techniques after the surface was covered with epoxy resin. A TEM bright field image was observed using a Hitachi H-9000 UHR at 300 kV under the (110) zone axis condition. Figure 1 shows a cross-sectional TEM micrograph of the Si wafer after grinding. The width of the damaged layer was 100–200 nm, and it included an amorphous layer and crystalline defects, such as stacking faults and dislocations. The observed defects were typical of those caused by grinding.[11,12] Small recess areas were covered with amorphous Si, and interference fringes and dislocation contrasts overlapped in the dark areas. Using selective area diffraction corresponding to the dark areas, split diffraction spots were observed in the [110] diffraction, but their spots did not represent a circular shape.[15] This indicates that the region with the dark contrast keeps the diamond structure including the slight distortion. To know annealing behavior of defects introduced by grinding, the samples were annealed in vacuum up to 1000 °C (30 min) using a conventional furnace annealing system.

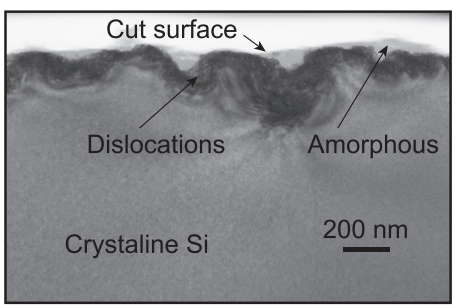

FIG. 1. Cross-sectional TEM micrograph of a Si wafer after grinding. Below a thin amorphous layer, a region of high density dislocation was introduced.

With a monoenergetic positron beam [direct current (DC) type] applied, Doppler broadening spectra of the annihilation radiation were measured with a Ge detector as a function of the incident positron energy E. The spectra were characterized by the S parameter, defined as the fraction of annihilation events over the energy range of 510.24–511.76 keV, and by the W parameter, defined as the annihilation events in the ranges of 506.44–508.72 keV and 513.28–515.56 keV. Doppler broadening profiles with 5×10^6 counts were also measured using a coincidence system.[13,14] The relationship between S and E was analyzed by VEPFIT, a computer program developed by van Veen *et al.*[16] The $S-E$ curve was fitted using

$$S(E) = S_s F_s(E) + \Sigma S_i F_i(E), \tag{1}$$

where $F_s(E)$ and $F_i(E)$ are the fractions of thermalized positrons annihilated at the surface and in the i-th layer, respectively; $(F_s(E) + \Sigma F_i(E) = 1)$. S_s and S_i are S parameters that correspond, respectively, to the annihilation of positrons at the surface and that of positrons in the i-th block. Details of the application of VEPFIT to the $S-E$ curves are described elsewhere.[17,18] All measurements were done after the removal of oxide layers using dilute HF.

The lifetime spectrum of positrons was measured using a pulsed monoenergetic positron beam. A brightness enhancement method was used to reduce the beam size at the sample to about 1 mm. Details of the positron focusing system are described elsewhere.[19] Approximately 3×10^6 counts were accumulated. The lifetime spectrum of positrons $S_{LT}(t)$ is given by

$$S_{LT}(t) = \sum \lambda_i I_i \exp(-\lambda_i t), \tag{2}$$

where λ_i and I_i are the annihilation rate and intensity of positrons of the i-th component, respectively ($\Sigma I_i = 1$). The lifetime of positrons τ_i is given by $1/\lambda_i$. The observed spectra were analyzed with a time resolution of approximately 260 ps (full-width at half-maximum: FWHM) using the RESOLUTION computer program.[20]

III. RESULTS AND DISCUSSION

We measured the S parameter of the Si wafer after grinding as a function of incident positron energy E. It was found that the S value saturated at $E > 20$ keV, suggesting that almost all positrons annihilate in the bulk within this energy range. Thus, the S value for this energy range is the one for defect-free (DF) Si. Figure 2 shows the S values normalized using the value of defect-free Si for the sample before and after annealing at typical temperatures. The mean implantation depth of positrons is shown on the upper horizontal axis. For the sample before annealing, the S value increased with decreasing E; the value then became almost constant at $E < 3$ keV, which corresponds to the trapping of

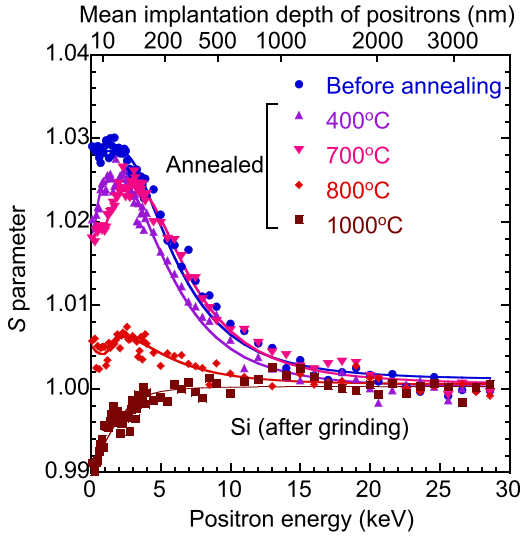

FIG. 2. *S* parameters as a function of incident positron energy *E* for the Si wafer after grinding. The *S* values were normalized using the value corresponding to the annihilation of positrons in defect-free Si. Results for annealed samples are also shown. The solid curves are fittings of the diffusion equation for positrons to the experimental data.

positrons by vacancy-type defects introduced by grinding. The observed $S-E$ curve was fitted using Eq. (1), and the solid curves in Fig. 2 are fits to the experimental data. In the fitting, the damaged region was divided into two layers (first and second layers) and the third layer was assumed to be the defect free area. For the samples annealed below 800 °C, the diffusion lengths of positrons in the damaged region were obtained to be 1–3 nm. These short diffusion lengths suggest that positrons implanted into the damaged region are fully trapped by vacancy-type defects.[21]

Figure 3 shows the derived depth distributions of *S* from the fitting of the $S-E$ curves shown in Fig. 2. For the sample before annealing, the width of the damaged layer was obtained as 98 ± 7 nm. From comparison between the damaged region observed by XTEM (Fig. 1) and the depth distribution of *S*, we attribute the large *S* value observed at $E < 3$ keV to not only the annihilation of positrons trapped

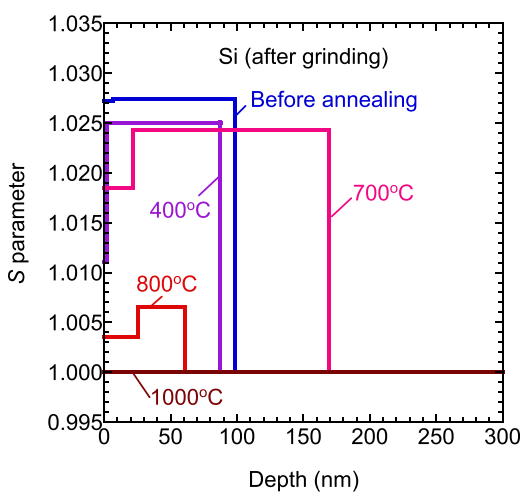

FIG. 3. Depth distributions of *S* for the samples before and after annealing derived from the fitting (Fig. 2).

by vacancy-type defects in the crystalline region but also to those in open spaces in the amorphous layer. The lifetime spectrum of a positron was measured at $E = 2$ keV. As shown in Figs. 1 and 2, the *S* values measured at $E = 2$ keV are close to the values of the damaged regions, suggesting that almost all positrons implanted with this energy range annihilate from the trapped state by defects. Thus, the effect of the positron annihilation at the surface is considered to be neglected in the analysis of the lifetime spectrum. The spectrum was decomposed into two components. The values of τ_1 and τ_2 were derived as 285 ± 9 ps and 490 ± 20 ps ($I_2 = 11 \pm 2\%$). It has been reported that positrons are trapped by relatively small vacancy-type defects which are closely related to dislocations and large vacancy clusters in plastically deformed Si.[22–24] The typical lifetimes of positrons trapped by those defects are about 300 ps and 500–600 ps, respectively. Thus, we can conclude that the observed annihilation characteristics of positrons in the damaged region for the sample before annealing is close to those for plastically deformed Si. Leipner *et al.*[24] attributed the short positron lifetime to the positron annihilation in small vacancy-type defects, such as monovacancies, *V*. According to another theoretical calculation,[25] the first lifetime is rather close to the lifetime of positrons trapped by divacancies, V_2 (299 ps). Since the structure of vacancy-type defects introduced in an area with high density dislocation networks is expected to be strongly influenced and relaxed by the stress caused by such dislocations, the modeling of the defect structure in the calculation is difficult. The longer lifetime component is attributed to large vacancy clusters ($>V_{18}$),[24] and they are considered to be introduced by interactions between dislocations. We will come back to this point later.

In the $S-E$ curve for the sample annealed at 400 °C, a decrease in the *S* value was observed within the measured energy range (0–30 keV); this was mainly due to the decreased vacancy concentration in the damaged region. This also suggests that the location of the vacancy-type defects was almost identical to that for the sample before annealing. For the sample annealed at 700 °C, although a decrease in *S* in the subsurface region ($E = 0$–4 keV) was observed, the *S* values at $E > 4$ keV were close to those for the sample before annealing, suggesting a shift of the damaged region toward the inside of the sample. As shown in Fig. 3, the depth distribution of vacancies for this sample reached 180 nm (Fig. 3).

Figure 4(a) shows annealing behaviors of the *S* value for the first and second layers (S_1 and S_2), and Fig. 4(b) shows the positions of the interfaces between the *i*-th and $(i+1)$th layers ($D_{i/i+1}$) ($i = 1$ and 2). For the sample annealed at 900 °C, the damaged region was represented using one layer. The values of S_1 and S_2 correspond to mainly the positron annihilation in amorphous and crystalline regions, respectively. The S_2 value represents mainly the annihilations of positrons trapped by the small vacancy-type defects and the vacancy clusters. In Fig. 4(a), the S_2 value decreased with increasing annealing temperature below 500 °C, but started to increase at 600 °C. The observed annealing behavior of S_2 was close to that of the mean positron lifetime τ_m for Si deformed at 800 °C,[24] where an increase in τ_m is observed

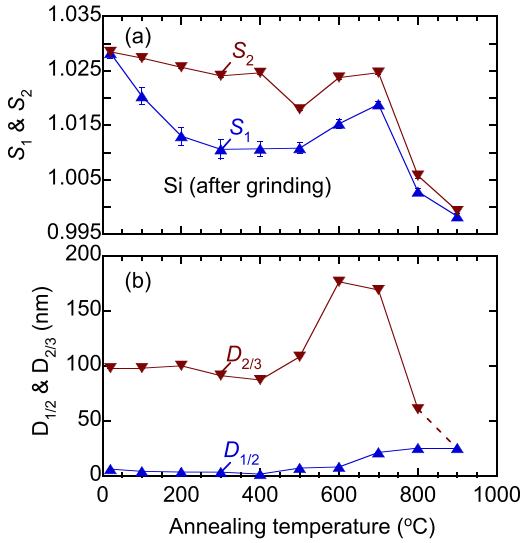

FIG. 4. (a) Annealing behavior of S and (b) the width of the damaged region introduced by grinding of the Si wafer. The damaged region was divided into two layers, where the S values in the i-th layer and the positions of the interfaces between the i-th and $(i+1)$-th layers are indicated as S_i and $D_{i/i+1}$ $(i=1$ and 2).

after annealing at 600 °C; we attributed this to rearrangements of dislocation networks and resultant emissions of vacancy-type defects.

It is well known that movements and interactions of dislocations generate defects. The primitive mechanism of point defect emission is the dragging of nonglissile jogs or superjogs of screw dislocations. When screw dislocations move along the primary glide plane, jogs are forced to climb by the gliding dislocations, and then emit point defects. Strings of point defects are left behind the jogs. If the deformation is done at a temperature higher than the annealing temperature for such defects, they could interact with each other and form vacancy or interstitial clusters. As shown in Fig. 4(b), the damaged region expanded to about 170 nm after annealing at 600 and 700 °C. This corresponds to the emission of vacancies caused by the dislocation motion, and their diffusion toward the inside of the sample. This means that the width of the damaged layer expands as the sample temperature increases to 600 °C if the residual damage introduced by grinding is not removed. The value of S started to decrease above 800 °C annealing, suggesting that the stability limit of the vacancies is likely to have been reached and they started to disappear.

For the sample before annealing, the vacancy clusters are considered to be introduced by the interaction of dislocations and the subsequent defect emission. Because the dislocation motion is suppressed at room temperature and the wafer cutting speed is far higher than that of the dislocation motion, they are believed to be relatively immobile.[12] The present results, however, suggest that the motion of dislocations and their concentration is high enough for dislocations to interact with each other and create vacancies. The formation of vacancy clusters requires the diffusion of pre-existing vacancies and their subsequent agglomeration, but these are also suppressed at room temperature. The total energy of monovacancy strings introduced by the jog dragging is expected to be decreased by the formation of vacancy clusters.[26] Because those interactions between vacancies would occur under a stress field from dislocations, the reactions could also be promoted by the presence of dislocations.[27]

Figure 5 shows the (S,W) values of coincidence Doppler broadening spectra measured at $E=2$ keV for the samples before and after annealing. These values were normalized using the (S,W) value corresponding to the annihilation of positrons in DF Si. Because the mean implantation depth of positrons with $E=2$ keV is 40 nm, these values can be mainly attributed to both the annihilations of positrons in the amorphous and crystalline regions. With increasing annealing temperature, the (S,W) values did not approach the value for the sample before annealing or move toward the value for DF; instead, the values went around the DF-value in a counter-clockwise direction (decreasing S and increasing W) as temperature increased. The S (W) value corresponding to the positron annihilation in oxide (SiO_2) layers or at the interface between SiO_2 and Si is known to be smaller (larger) than the value for the annihilation of positrons from DF-Si.[28,29] In the present work, however, because the measurements for the annealed samples were done after HF-etching, the effect of oxides on the (S,W) value can be neglected. It was reported that oxygen incorporation with vacancy-type defects decreases (increases) S (W) value, which is attributed to the annihilation of positrons with the high-momentum electron of oxygen.[30] Thus, the observed successive variation of the defect species can be attributed to an interaction between oxygen and vacancy-type defects. For the samples annealed at 800–900 °C, the residual damaged layer was located at <25 nm, and this is considered to be the amorphous layer introduced by phase transition. Thus, upon the re-crystallization of this region, vacancy-oxygen complexes are considered to be introduced. In Fig. 4(a), therefore, the value of S_1 value is considered to be strongly affected by oxygen in the amorphous layer.

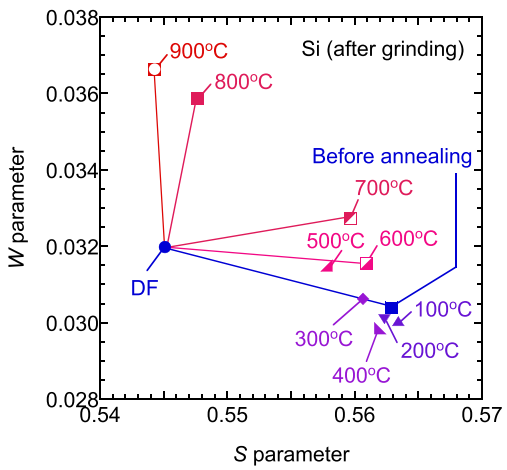

FIG. 5. (S,W) values for the damaged region in the Si wafer after grinding. These values were normalized using the (S,W) value corresponding to the annihilation of positrons in DF Si. Annealing temperatures are shown in the figure. The (S,W) value for DF-Si is also shown. Arrows show the effect of the annealing on the (S,W) value.

IV. SUMMARY

We used monoenergetic positron beams to study vacancy-type defects introduced by grinding of Si wafers. Doppler broadening spectra were measured using a monoenergetic positron beam as a function of the incident energy of positrons for the sample before and after annealing. Coincidence Doppler broadening spectra were also measured. Lifetime spectra of positrons were measured using a pulsed monoenergetic positron beam. The depth of the vacancy-rich region introduced by grinding was determined to be 98 nm, where the major species were identified as (i) relatively small vacancy-type defects incorporated in dislocations and (ii) large vacancy clusters. For annealing below 400 °C, no large shift of the vacancy-rich region was observed. In this temperature range, the *S* value decreased with increasing annealing temperature, suggesting a decrease in the concentration of vacancies. With 600 and 700 °C annealing, the defect-rich region expanded to about 180 nm, which was attributed to the rearrangement of dislocation networks, and the resultant emission of point defects towards the inside of the sample. Above 800 °C annealing, the stability limit of those vacancies was reached and they started to disappear. After annealing out the vacancy-type defects (900 °C), oxygen-related defects were introduced below the surface (<25 nm). We have shown that the positron annihilation parameters are sensitive to vacancy-type defects introduced by mechanical grinding of semiconductor wafers, and that positron annihilation spectroscopy is a useful tool for controlling wafer thinning conditions before the CMP process.

ACKNOWLEDGMENTS

Part of this work was implemented under the WOW alliance and the WOW Research Center Co. We would like to thank Disco Corporation for wafer thinning and Toray Research Center Inc. for TEM observation.

[1]M.-F. Lai, S.-W. Li, J.-Y. Shih, and K.-N. Chen, Microelectron. Eng. **88**, 3282 (2011).
[2]J. F. Gibbons and K. F. Lee, IEEE Trans. Electron Devices Lett. **1**, 117 (1980).
[3]S. Kawamura, N. Sasaki, T. Iwai, M. Nakano, and M. Takagi, IEEE Trans. Electron. Devices Lett. **4**, 366 (1983).
[4]M. Koyanagi, H. Kurino, K. W. Lee, K. Sakuma, N. Miyakawa, and H. Itani, IEEE Micro. **18**, 17 (1998).
[5]K. W. Lee, T. Nakamura, T. Ono, Y. Yamada, T. Mizukusa, H. Hashimoto, K. T. Park, H. Kurino, and M. Koyanagi, IEEE Tech. Dig. – Int. Electron Devices Meeting **2000**, 165.
[6]N. Maeda, H. Kitada, K. Fujimoto, K. Suzuki, T. Nakamura, and T. Ohba, in *Advanced Metallization Conference* (Materials Research Society, 2009), p. 501.
[7]Y. Mizushima, H. Kitada, K. Koshikawa, S. Suzuki, T. Nakamura, and T. Ohba, Jpn. J. Appl. Phys., Part 1 **51**, 05EE03 (2012).
[8]E. Brinksmeier, Precision Eng. **11**, 211 (1989).
[9]T. Abe, Precision Eng. **13**, 251 (1991).
[10]Z. J. Pei, S. R. Billingsley, and S. Miura, Int. J. Mach. Tools Manuf. **39**, 1103 (1999).
[11]Z. J. Pei, G. R. Fisher, and J. Liu, Int. J. Mach. Tools Manuf. **48**, 1297 (2008).
[12]J. Yan, T. Asami, H. Harada, and T. Kuriyagawa, Precision Eng. **33**, 378 (2009).
[13]R. Krause-Rehberg and H. S. Leipner, *Positron Annihilation in Semiconductors, Solid-State Sciences* (Springer-Verlag, Berlin, 1999), Vol. 127.
[14]F. Tuomisto and I. Makkonen, Rev. Mod. Phys. **85**, 1583 (2013).
[15]Y. Mizushima, Y. Kim, T. Nakamura, R. Sugie, H. Hashimoto, A. Uedono, and T. Ohba, Jpn. J. Appl. Phys4 **53**, 05GE04 (2014).
[16]A. van Veen, H. Schut, J. de Vries, R. A. Hakvoort, and M. R. Ijpma, AIP Conf. Proc. **218**, 171 (1991).
[17]A. Uedono, S. Ishibashi, T. Ohdaira, and R. Suzuki, J. Cryst. Growth **311**, 3075 (2009).
[18]A. Uedono, S. Ishibashi, N. Oshima, and R. Suzuki, Jpn. J. Appl. Phys., Part 1 **52**, 08JJ02 (2013).
[19]N. Oshima, R. Suzuki, T. Ohdaira, A. Kinomura, T. Narumi, A. Uedono, and M. Fujinami, Appl. Phys. Lett. **94**, 194104 (2009).
[20]P. Kirkegaard, M. Eldrup, O. E. Mogensen, and N. J. Pedersen, Comput. Phys. Commun. **23**, 307 (1981).
[21]A. Uedono, S. Tanigawa, T. Ohshima, H. Itoh, M. Yoshikawa, I. Nashiyama, T. Frank, G. Pensl, R. Suzuki, T. Ohdaira, and T. Mikado, J. Appl. Phys. **87**, 4119 (2000).
[22]R. Krause-Rehberg, M. Brohl, H. S. Leipner, Th. Drost, A. Polity, U. Beyer, and H. Alexander, Phys. Rev. B. **47**, 13266 (1993).
[23]A. Kawasuso, M. Suezawa, M. Hasegawa, S. Yamaguchi, and K. Sumino, Jpn. J. Appl. Phys., Part 1 **34**, 4579 (1995).
[24]H. S. Leipner, V. V. Mikhnovich, Jr., V. Bondarenko, Z. Wanga, H. Gu, R. Krause-Rehberg, J.-L. Demenet, and J. Rabier, Physica B **340–342**, 617 (2003).
[25]M. Hakala, M. J. Puska, and R. M. Nieminen, Phys. Rev. B **57**, 7621 (1998).
[26]H. S. Leipner, C. G. Hűbner, T. E. M. Staab, M. Haugk, A. Sieck, R. Krause-Rehberg, and T. Frauenheim, J. Phys.: Condens. Matter **12**, 10071 (2000).
[27]T. Wider, S. Hansen, U. Holzwarth, and K. Maier, Phys. Rev. B. **57**, 5126 (1998).
[28]A. Uedono, L. Wei, S. Tanigawa, R. Suzuki, H. Ohgaki, T. Mikado, and Y. Ohji, J. Appl. Phys. **75**, 3822 (1994).
[29]M. P. Petkov, K. G. Lynn, and A. van Veen, Phys. Rev. B **66**, 045322 (2002).
[30]A. Uedono, Z. Q. Chen, A. Ogura, R. Suzuki, T. Ohdaira, and T. Mikado, J. Appl. Phys. **91**, 6488 (2002).